

Techniques for testing in-service materials using portable indentation systems have been developed for more than 15 years. In one disadvantage, the techniques use material-specific parameters to determine yield strength of an unknown material, which must be premeasured from tensile testing of the material.



Tests prove indentation technique for assessment of in-service line pipe

Yeol Choi
Jae-il Jang
Joon Park
Frontics Inc.
Seoul

Dongil Kwon
Seoul National University
Seoul

Ming Gao
PII Pipeline Solutions,
GE Power Systems
Houston

Richard Kania
PII Pipeline Solutions,
GE Power Systems
Calgary

Advances in fundamental understanding of materials' mechanical behaviors have made it possible to overcome this disadvantage. Limitations of a maximum strain of 0.2 in./in. have also been removed as a result of improvement of the analysis methodology.

Other improvements, such as unloading curve analysis and pile-up and sink-in-effective quantification, have increased the accuracy of flow-curve analysis and tensile-property evaluation.

In addition to the principles of these improvements, this article presents the results of blind tests with three representative metallic materials compared with those of uniaxial tensile tests.

Also presented are the results of field measurements that demonstrate the effectiveness and reliability of the advanced system developed. Applications of the developed techniques to integrity assessment of welded structures are also discussed.

Mechanical properties

Integrity assessment and cost-effective management of in-service structures require that the mechanical properties of the structure's material be known.

Lack of documentation on pipeline materials, which is common for many older pipelines, results in the need for reestablishing the maximum allowable operating pressure for the pipeline via tensile testing or using a minimum

yield strength of 24 ksi or less.¹ In many cases, the use of this assumed minimum yield strength will lead to a very conservative assessment and result in needless and costly maintenance.

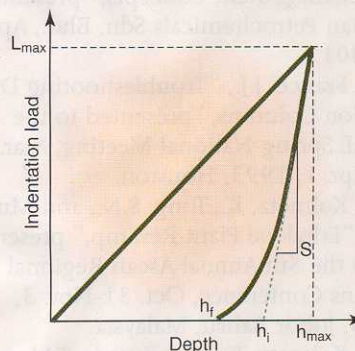
For tensile testing, US 49 CFR 192 specifies that one set of tensile tests must be done for each 10 lengths of pipe for pipelines of more than 100 pipe lengths. Because samples must be removed from the pipeline, the practice is both destructive and expensive.

Therefore, the instrumented indentation technique has emerged as one of the most practical and useful technologies for non-destructive, quantitative measurement of mechanical properties for in-field service structures.

Techniques for testing in-service materials using advanced portable indentation systems have been developed and used for several years.²⁻⁶ One of the systems uses universal correlation factors to determine yield strength of an unknown material, which must be pre-

INDENTATION TEST

Fig. 1



measured from tensile testing of the material.² It has been determined that the use of such universal factors can produce inconsistent results.⁴

During extensive testing of the technique,^{2,4} however, a correlation has been determined which allowed minimizing the differences between indentation predictions and API 5L tensile testing results.⁴ Further advances in the fundamental understanding of the mechanical behavior of materials made it possible to develop a more accurate process for yield-strength determination.^{3,6,7}

Limitations such as a maximum true

EQUATIONS

$$h_c^* = h_{\max} - \omega(h_{\max} - h_i) \quad (1)$$

$$L = K(h - h_i)^m \quad (2)$$

$$c^2 = \frac{a^2}{a^{*2}} = \frac{5(2 - n)}{2(4 + n)} \quad (3)$$

$$a^2 = \frac{5(2 - n)}{2(4 + n)} (2Rh_c^* - h_c^{*2}) \quad (4)$$

$$P_m = \frac{L_{\max}}{\pi a^2} \quad (5)$$

$$\epsilon_R = \frac{\alpha}{\sqrt{1 - (a/R)^2}} \frac{a}{R} \quad (6)$$

$$\frac{P_m}{\sigma_R} = \psi \quad (7)$$

$$L_r = \frac{\sigma_{ref}}{\sigma} \quad (8)$$

$$K_f = \frac{K_l}{K_{met}} \quad (9)$$

$$K_r = \left(\frac{E\epsilon_{ref}}{L_r\sigma_Y} + \frac{L_r^3\sigma_Y}{2E\epsilon_{ref}} \right)^{-0.5} \quad (10)$$

$$L_{r,\max} = \frac{\sigma_{flow}}{\sigma_Y} = \frac{(\sigma_Y + \sigma_U)/2}{\sigma_Y} \quad (11)$$

plastic strain of 0.2 in./in. that could be achieved for indentation systems have also been removed due to improvement of the analysis methodology. Other improvements in areas such as unloading-curve analysis and pile-up and sink-in-effective quantification, have been made which further increase the accuracy of tensile-property evaluation.^{3,6,7}

Deformation process

The advanced indentation technology has been developed from the conventional hardness test. This technology measures the indentation load and penetration depth during loading and unloading of a spherical indenter at constant speed, instead of the direct observation and measurement of indent size in the conventional hardness test.^{2,6-8}

DEFORMATION

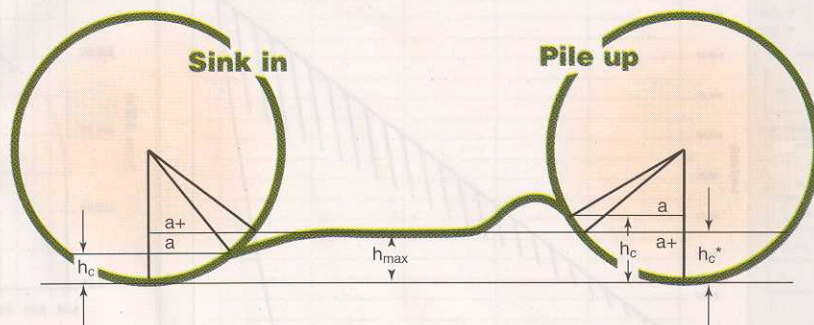


Fig. 2

An indentation load-depth curve is obtained from this procedure similar to the load-displacement curve from the uniaxial tensile test. This curve represents the deformation behavior of the test sample beneath the rigid ball indenter.^{2,3}

The equivalent true stress and strain identical with the flow properties from the standard uniaxial tensile test can be predicted on the analysis of indentation load-depth curve considering the indentation stress fields and deformation shape.^{6,7}

There are three stages of deformation in the indentation process: elastic, elastic-plastic, and fully plastic.⁸

A reversible deformation occurs at low load indentation in Stage I. When the indentation stress fields satisfy the yield criterion, a plastic zone arises near the indenter inside the material and expands to free surface, Stage II. In this stage, the mean contact pressure beneath the spherical indenter increases rapidly.

Finally, the hemispherical plastic zone grows into its surrounding elastic zone with a constant velocity as the indenter penetration depth increases, Stage III. The mean contact pressure slightly increases in the fully plastic region.

This three-stage deformation process is similar to the work-hardening behavior of the uniaxial tensile test except for nonhomogeneity

Predicting the uniaxial flow properties from indentation-induced deformation is described presently. The raw data from the indentation test are the indentation load-depth curve shown in Fig. 1

where only the load-depth curve in Stage III appears because of the limitation of the instrument resolution. Fig. 2 shows the elastic and plastic deformation around the indenter.

The equivalent stress and strain were defined in terms of the measured indentation contact parameters, such as contact depth, indenter shape, and the morphology of the deformed sample surface. The real contact properties are determined by considering both the elastic deflection and the material pile-up around the contacting indenter (Fig. 2).

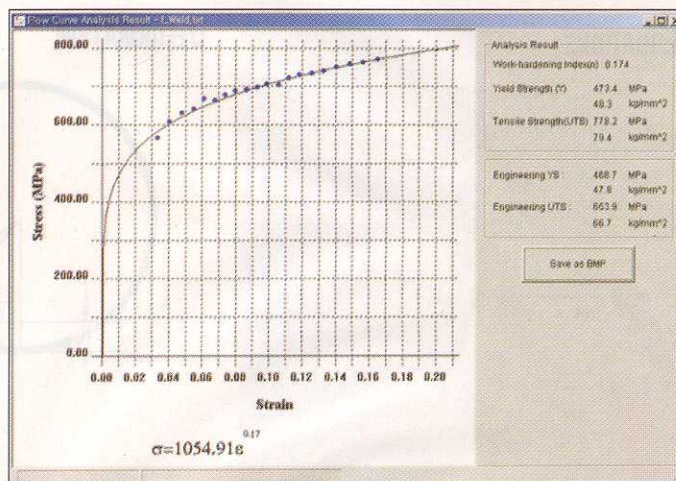
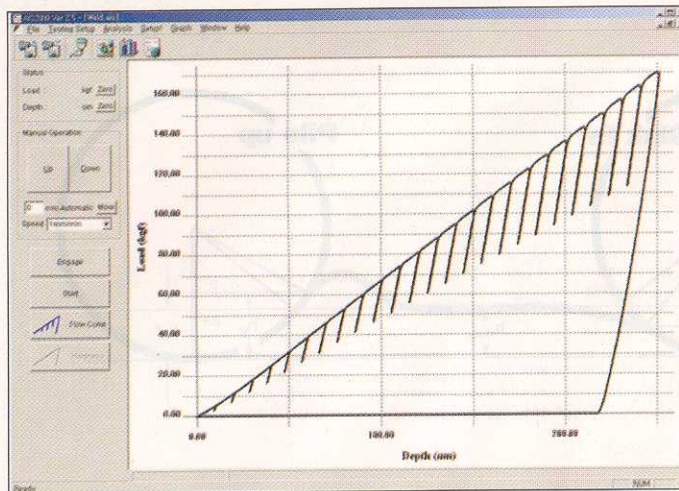
This analysis procedure is crucial. The predicted strength values would be either overestimated or underestimated significantly if this were not considered in the analysis.

The contact depth at maximum indentation load can be evaluated by analyzing the unloading curve with the concept of indenter geometry and elastic deflection, as shown in Equation 1 in the accompanying equations box.⁹

As shown in Fig. 1, h_i is the intercept indentation depth; the indenter shape parameter (ω) is 0.75 for the spherical indenter.

For h_i determination, initial unloading stiffness (S) is shown in Fig. 1 and obtained with the simple power law relation (Equation 2)⁸ where K , m , and h_i are determined by a least squares fitting procedure.

Then the initial unloading slope S is found by differentiating this equation and calculating the derivative at the maximum load and depth. Compared with linear regression analysis of each



Typical results of each test show load-depth curves from indentation tests (Fig. 3a, photo on left) and true stress-true strain curves converted from load-depth curves (Fig. 3b, photo on right).

partial unloading curve,² this power law fitting analysis has the advantages that it can reduce creep sensitivity and measured stiffness variation according to unloading portion analyzed.

The material pile-up around the indentation enlarges the contact radius from the analysis of elastic deflection. The extent of this pile-up is determined by a constant (c) and the work-hardening exponent (n) for steels in Equation 3^{10,11} where " a " is the real contact radius and a^* is the contact radius without considering the pile-up

around the indentation.

Using the geometrical relationship of the spherical indenter, the real contact radius is expressed in terms of indenter radius (R) and (h_c^*), as in Equation 4.

The contact mean pressure (P_m) is then expressed as Equation 5.

An equivalent strain (ϵ_R) of indentation is evaluated from the material displacement beneath the indenter, along the axis of indentation, and is a function of the real contact radius " a " multiplied by a fitting constant α in Equation 6. The value of α was determined

as 0.1 for various steels.⁶⁻⁸

In the case of metals including structural steels, the elastic and elastic-plastic deformation stages occurred at very low indentation load. Therefore, only the plastic-deformation region is considered in this study. The equivalent stress (σ_R) can be evaluated using the relationship with contact mean pressure (Equation 7)⁶⁻⁸ where Ψ is a constraint factor for plastic deformation with an upper limit of about 3 for fully plastic deformation of steels.

The exact values of work-hardening exponent, equivalent stress, and strain are calculated by iteration methods.⁶⁻⁷

From the analysis of each unloading curve as shown in Fig. 3a, both equivalent stress and strain values are determined.

The stress and strain relation is fitted as the power-type Hollomon equation¹² expressing work-hardening behavior, as shown in Fig. 3b.

The fitted curve is extrapolated to initial yield and ultimate tensile regions. Then, yield strength can be predicted through the Hollomon equation by extrapolating strain to the low-strain regime. The ultimate tensile strength was evaluated with the concept that uniform elongation is equal to the work-hardening exponent.¹²

Based on the fundamental understanding of the indentation-deformation process and the analysis procedure



Technicians use AIS 2000 in the field (Fig. 4).

RESULTS OF UNIAXIAL TENSILE, ADVANCED INDENTATION TESTS

Table 1

Materials	Tensile properties	Average values obtained		
		Two tensile tests	Four indentation tests	Difference, %
A12012	YS (MPa)	333.5	332.5	0.3
	UTS (MPa)	484.8	481.6	0.6
	Work hardening index	0.137	0.140	2.7
SS400	YS (MPa)	284.1	284.1	0.0
	UTS (MPa)	530.4	566.4	6.8
	Work hardening index	0.228	0.222	2.4
SCM4	YS (MPa)	684.1	641.3	6.3
	UTS (MPa)	971.6	923.0	5.0
	Work hardening index	0.130	0.139	6.6

developed previously, prediction of the yield strength for an unknown material no longer relies on the parameters that must be determined by tensile testing of the same material,² and the accuracy of the prediction is significantly improved as well.

Lab verification

To appraise the reliability and reproducibility of the test results in this procedure, tests compared the tensile properties obtained from the advanced indentation tests with those from uniaxial tensile tests.

The comparisons were made in a blind test of three representative metallic materials: SS400 steel (low-strength steel), SCM4 steel (high-strength steel), and Al-2012 (nonferrous metal).

While the tensile properties of each material were measured twice with an Instron 5582 uniaxial tensile tester, (Instron Corp., Canton, Mass.), the same target properties were measured four times with an Advanced Indentation System AIS-2000 (Frontics Inc.), using the procedure described.

Fig. 3 illustrates the typical results of each test, showing load-depth curves from indentation tests (Fig. 3a) and true stress-true strain curves converted from load-depth curves (Fig. 3b). All samples demonstrate good repeatability of the true stress-true strain curves from tensile tests.

The tensile properties measured by indentation tests are compared with those from uniaxial tensile tests (Table 1). The comparison shows the Advanced Indentation System testing pro-

vides accurate tensile properties.

Commercial API 5L-X65 pipelines of 762 mm OD and 17.5 mm WT that are generally used in Korea as natural gas transmission pipelines were studied.

A portable (AIS-2000) was used for yield and ultimate tensile-strength measurements.

The maximum capacity of the load sensor of the system is 3,000 N (Newton). The maximum displacement of the displacement sensor (a linear variable differential transformer, LVDT) is 3 mm. The accuracy of each of the sensors is 3 N and 0.2 μm , respectively. The LVDT is installed next to the inden-

TENSILE PROPERTIES FROM ADVANCED INDENTATION, UNIAXIAL TENSILE TESTS*

Table 2

Location	Tensile properties	Uniaxial tensile test	Advanced indentation test
A	YS (MPa)	488	487
	UTS (MPa)	674	673
	Work hardening index	0.143	0.153
B	YS (MPa)	485	489
	UTS (MPa)	654	656
	Work hardening index	0.163	0.162

*Line pipe API X-65.

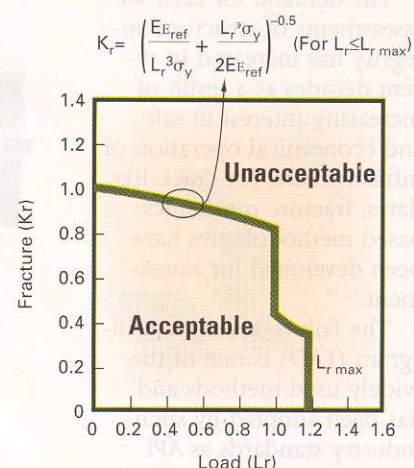
ter. The 0.5-mm (diameter) spherical WC indenter was an integrated part of the WC stem, which eliminated brazing of the WC indenter to the steel stem.

With this type of arrangement, the accurate data of load and depth during indentation can be obtained without the error of system compliance from the equipment.

Because unreliable attachment of the system to the pipeline could result in significant errors in load and displacement measurements, a pair of customer-made curved magnets, along

TYPICAL FAD

Fig. 5



with a mechanical chain, were used to firmly attach the system to the pipe. Fig. 4 shows the AIS 2000 in use at an in-service field location.

Considering microstructural variations in the pipe, three to four indentations were made and average tensile properties obtained. The distance between indentation marks was 3 mm to avoid the superposition of plastic deformation fields.

To verify the accuracy of the data obtained, material in the indented areas was removed and machined for uniaxial tensile tests, which were performed in accordance with ASTM E8.¹³

Table 2 shows the results obtained from the advanced indentation method and standard tensile test for two locations, A and B, along the pipeline. The agreement between these two methods was excellent.

Additional tests were performed on two sections of pipeline made of Grade B and X-52 steel. Again, agreement between the advanced indentation method and tensile tests from mill certifications was excellent.¹⁴ In-field tensile property evaluations of API X-42, X-60 pipelines in Mexico were performed with an AIS 2000 system to verify the reliability and repeatability of the techniques developed.

Application

The demand for accurate assessments of structural integrity has increased in recent decades as a result of increasing interest in safe and economical operation of infrastructure. For crack-like flaws, fracture mechanics-based methodologies have been developed for assessment.¹⁵⁻¹⁸

The failure-assessment diagram (FAD) is one of the widely used methods and has been adopted by such industry standards as API 579 and BS 7910:1999. The FAD method combines the brittle fracture and plastic collapse for the assessment in one diagram and provides different assessment levels based on the required conservatism and availability of material property.

Each FAD code¹⁹⁻²² has higher-level FADs that require finite-element methods (FEM) for J-integral analysis. In practice, however, they have rarely been used in the field because of the difficulty of assessing the reliability of the FEM results.

Therefore, the material-specific FAD, such as Level 2B of BS7910, Level 3B of API 579, Option 2 of R6, and Level 3 of SINTAP,¹⁹⁻²² is desirable because it is a less conservative but cost-effective method in industrial practice if the required material property information becomes available.

Fig. 5 is a typical material-specific FAD used in current codes for fitness for service (FFS) assessment of crack-like flaws. L_r and K_r are the respective ratios of load and fracture toughness in Equations 8 and 9 where σ_{ref} , σ , K_I , and K_{mat} are reference stress, applied stress, stress intensity factor, and material's fracture toughness, respectively.

The criterion line of material-specific FAD, i.e. the failure-assessment curve (FAC), is given by Equation 10 where: ϵ_{ref} = the reference strain defined as the true strain corresponding to a reference stress. In Equation 10, σ_Y and E

PIPE SECTION WITH CRACK

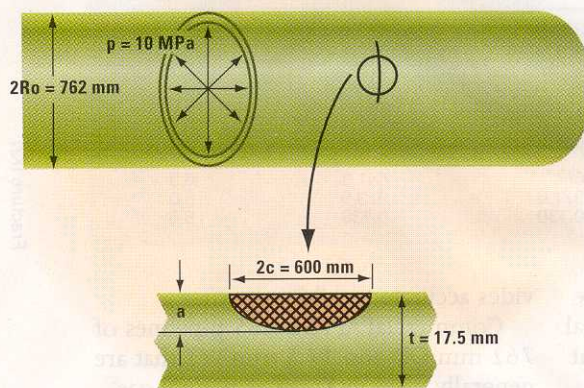


Fig. 6

FAD FOR THREE CRACK DEPTHS

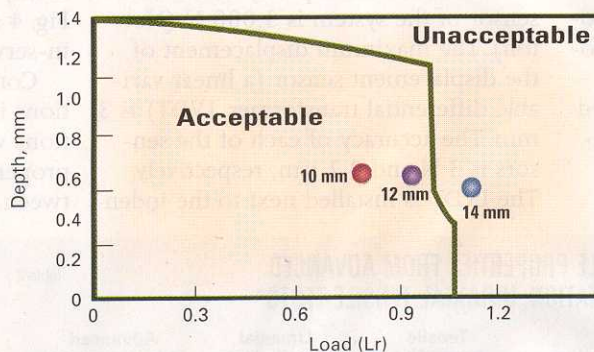


Fig. 7

are the yield strength and elastic modulus, respectively.

Cracks with their (K_r , L_r) values inside FAC are acceptable. Cracks with their (K_r , L_r) values outside FAC are unacceptable and become critical if their (K_r , L_r) values equal to those predicted by Equation 10.

To determine the FAC curve and the L_r and K_r values of cracks, material properties such as yield strength and fracture toughness (Equations 8 and 9) are required. Additionally, the ultimate tensile stress is also required to define $L_{r,max}$, the limit value of plastic collapse, with Equation 11, where σ_{flow} and σ_U are flow stress and ultimate tensile stress, respectively.

Therefore, the tensile properties, including true stress-true strain curve, yield, and ultimate tensile strength of

the material near the crack-like flaw, are critical input parameters in assessing fitness-for-service according to current FAD codes. In most cases, however, these values are not available.

If the tensile properties of the material near the crack can be measured nondestructively in the field and used as input data for FAD construction, the assessment results can be more accurate than those using mill sheet data or specified minimum yield strength (SMYS).

The advanced indentation technique provides an effective tool to support the material-specific based FAD assessment of crack-like flaws in the pipeline, not only for the base material but also for weld and heat-affected zones.

An example illustrates the effectiveness of the developed approach.

Fig. 6 is a schematic of a section of the pipe (762 mm OD x 17.5 mm WT) and a virtual circumferential crack (a fixed length of 600 mm with varied depth). Only an internal pressure of 10 MPa is assumed.

To construct a material specific FAD (API 579 Level 3B), all mechanical properties required were determined with AIS-2000, except the fracture toughness value (which cannot be determined using the indentation method) that was determined from the previously research on the same material.

Fig. 7 shows the constructed FAD and the assessment result for three different depths of cracks (the length of the crack is the same, i.e., 600 mm long). The FAD suggests that cracks with depths of 10 and 12 mm are acceptable, while the crack with its depth of 14 mm is unacceptable. The critical flaw size is between 12 and 14 mm.

More details of the material specific FAD approach using the advanced indentation technique is discussed elsewhere.²³ ♦

References

1. US Federal Pipeline Safety Standard 49 CFR 192, Section IID of Appendix B.
2. Haggag, F.M., "Nondestructive Determination of Yield Strength and Stress-Strain Curves of In-Services Transmission Pipelines Using Innovative Stress-Strain Microprobe Technology," ATC Report, ATC/DOT/990901.
3. Field, J.S., and Swian, M.V., "Determining the Mechanical Properties of Small Volumes of Material from Submicrometer Spherical Indenter," *Journal of Materials Research*, Vol. 10, pp. 101-12, 1995.
4. Russell, A.D., Jones, B.L., and Manning, L., "Determining the In-Situ Tensile Properties of Pipelines Using the Automated Ball Indentation (ABI) Technique," to be published, 2003.
5. Jellard, P., Kirkwood, M., Balmer, Derek, and Collingwood, Phil, "Georgian Pipeline Company Upgrading An Old Russian Pipeline," PII Total Integrity Conference, Prague, May 20-22, 2002.
6. Ahn, J.H., Choi, Y., and Kwon, D., "Evaluation of Plastic Flow Properties of Materials Through the Analysis of Indentation Load-Depth Curve," *Journal of the Korean Institute of Metal and Materials*, Vol. 38, pp. 1606-11, 2000.
7. Ahn, J.H., and Kwon, D., "Derivation of Plastic Stress-Strain Relationship from Ball Indentation: Examination of Strain Definition and Pileup Effect," *J. Mater. Res.*, Vol. 16 (2001), pp. 3170-78.
8. Francis, F.A., "Phenomenological Analysis of Plastic Spherical Indentation," *Journal of Engineering Materials and Technology Transaction ASME*, Vol. 98, pp. 272-81, 1976.
9. Oliver, W. C., and Pharr, G.M., "An Improved Technique for Determining Hardness and Elastic Modulus Using Load and Displacement Sensing Indentation Experiment," *Journal of Materials Research*, Vol. 7, pp. 1564-83, 1992.
10. Norbury, A.L., and Samuel, T., "The Recovery and Sinking-In or Piling-Up of Material in the Brinell Test, and the Effects of These Factors on the Correlation of the Brinell With Certain Other Hardness Tests," *Journal of Iron and Steel Institute*, Vol. 117, pp. 673-87, 1928.
11. Hill, R.F.R.S., Storåkers, B., and Zdunek, A., "A Theoretical Study of the Brinell Hardness Test," *Proceedings of Royal Society in London*, Vol. A423 (1989), pp. 301-30, 1989.
12. Dieter, G.E., *Mechanical Metallurgy*, London: McGraw-Hill, 1988; pp. 283-92.
13. ASTM E8-91: Standard Test Methods of Tensile Testing of Metallic Materials, Philadelphia: American Society of Testing and Materials, 1991.
14. Kania, Richard, and Gao, Ming, "A Comparison of the Test Results of Tensile Properties Between AIS 2000 Measurements and Mill Certificates," PII USA, 2002.
15. Zerbst, U., Heerens, J., and Schwalbe, K-H., "The Fracture Behavior of a Welded Tubular Joint—an ESIS TC1.3 Round Robin on Failure Assessment Methods Part I: Experimental Data Base and Brief Summary of the Results," *Eng. Frac. Mech.*, Vol. 69 (2002), pp. 1093-1100.
16. Milne, I., Ainsworth, R.A., Dowling, A.R., and Stewart, A.T., "Background and Validation of CEBG Report R/H/R-6 Revision 3," *Int. J. Press. Vessel Piping*, Vol. 32, pp. 105-96, 1988.
17. Ainsworth, R.A., Gutierrez-Solona, F., and Ruiz Ocejio, J., "Analysis Levels Within the SINTAP Defect Assessment Procedure," *Eng. Frac. Mech.*, Vol. 67 (2000), pp. 515-27.
18. Anderson, T.L., and Osage, D.A., "API 579: A Comprehensive Fitness-For-Service Guide," *Int. J. Press. Vessel Piping*, Vol. 77 (2000), pp. 953-63.
19. R-6, Assessment of the Integrity of Structures Containing Defects, British Energy, R/H/R-6-Revision 3, 1998.
20. BS7910, "Guide and Methods for Assessing the Acceptability of Flaws in Fusion Welded Structures," British Standards Institution, 1999.
21. SINTAP, "Structural Integrity Assessment Procedures for European Industries, Final Procedure," Brite-Euram Project Number BE95-1426, 1999.
22. API 579, "Recommended Practice for Fitness for Service," Washington: American Petroleum Institute, 2000.
23. Jae-il Jang, et al., "Instrumented Indentation Technique to Measure Flow Properties: A Novel Way to Enhance the Accuracy of Integrity Assessment," *Proceedings of the 22nd International Conference on Offshore Mechanics and Arctic Engineering*, June 8-13, 2003, Cancun.

The authors

Yeol Choi (ychoi@frontics.com) is chief technical officer of Frontics Inc., Seoul. He holds an MS (2000) in materials science and engineering from and is a doctoral candidate at Seoul National University. He is a member of the American Society of Testing and Measurement.

Jae-il Jang is a senior researcher for Frontics and holds an MS (1994) and PhD (2000) in materials science and engineering from Seoul National University.

Joon Park is president of Frontics and holds an MS (1995) in materials science and engineering from Seoul National University.

Dongil Kwon is director of the National Research Laboratory for the NanoAssessment and MicroReliability Laboratory at Seoul National University where he also holds the rank of professor. He obtained a PhD (1987) from Brown University and is a member of ASTM.

Ming Gao is a senior integrity advisor and chief engineer for integrity services for PII Pipeline Solutions, GE Power Systems Oil & Gas in Houston. Gao holds a PhD (1983) from Lehigh University and is a member of ASTM, ASM, ASME, and NACE.

Richard Kania is an integrity services project manager for PII North America, GE Power Systems, Oil & Gas in Calgary. He holds a masters of engineering degree (1994) in Management and is a registered professional engineer in the Province of Alberta. Kania is a member of ASTM.